Westward Propagating Normal Modes in the Presence of Stationary Background Waves

GRANT BRANSTATOR

*National Center for Atmospheric Research, * Boulder, Colorado*

ISAAC HELD

Geophysical Fluid Dynamics Laboratory, Princeton University, Princeton, New Jersey

(Manuscript received 27 April 1993, in final form 6 June 1994)

ABSTRACT

Eigenvectors and eigenvalues of the nondivergent barotropic vorticity equation linearized about zonally asymmetric wintertime mean flows are calculated to determine which barotropic modes might contribute to westward propagating disturbances observed in nature. Of particular interest are modes that correspond to a recurring pattern concentrated in the Western Hemisphere with a period of about 25 days reported by Branstator and Kushnir.

The most unstable modes of November–March means from individual years tend to be westward propagating and have a structure that is similar to the observed 25-day pattern.

By following the evolution of each Rossby–Haurwitz mode as the basic state is gradually changed from a state of rest to an observed mean state, it is demonstrated that all but about eight of the Rossby–Haurwitz modes will be modified beyond recognition by the action of the time mean flow. One of these, the second gravest antisymmetric zonal wavenumber-one mode (denoted {1, 3} and sometimes referred to as the 16-day wave), has a structure that bears some resemblance to the observed 25-day pattern, but it is typically neutral. The structural similarity between this mode and the 25-day pattern is not as pronounced as the similarity between the most unstable modes and the 25-day pattern. Furthermore, the mode for the observed basic state that {1, 3} evolves to depends on the path by which the resting state is transformed into the observed state, suggesting that {1, 3} cannot always be thought of as a distinct mode in the presence of a realistic background. The results indicate that even if {1, 3} can be considered to exist in wintertime mean flows, it is distinct from the most unstable modes on those flows.

By slowly changing the basic states that support the westward propagating unstable modes until they are equal to the climatological January state that earlier studies have shown produces quasi-stationary teleconnection-like modes, it is demonstrated that the unstable westward propagating and quasi-stationary modes are related to each other.

1. Introduction

Perturbations that resemble external Rossby normal modes have been isolated from large-scale tropospheric and stratospheric variability in a variety of studies. Based on this body of work, which has been reviewed by Madden (1979), Salby (1984), Ahlquist (1985), and Venne (1989), many westward propagating disturbances in nature are generally thought to be manifestations of these classical modes. In this paper we examine whether this identification continues to be justified if one takes into account the climatological stationary waves with their potential to distort or act as a source of energy to perturbations.

The best documented connection between Rossby normal-mode theory and observations is probably that between the observed "5-day wave" and the gravest symmetric wavenumber one mode {1, 1}.[1] Of more meteorological interest is the proposed connection between the observed "16-day wave" and the second symmetric wavenumber one mode, {1, 3}. For example, it has been argued by Madden and Labitzke (1981) that the 16-day wave played a dominant role in the

* The National Center for Atmospheric Research is sponsored by the National Science Foundation.

Corresponding author address: Dr. Grant W. Branstator, Global Dynamics Section, National Center for Atmospheric Research, P.O. Box 3000, Boulder, CO 80307-3000.

[1] The notation for external Rossby normal modes is not uniform. We use $\{m, n\}$, where m is the zonal wavenumber and $n - 1$ the number of zeroes in the pressure from pole to pole. The odd n modes are referred to as *symmetric*, having symmetric geopotential and zonal winds but antisymmetric streamfunction. In a nondivergent barotropic model linearized about solid body rotation, $\{m, n\}$ has a streamfunction with the horizontal structure of the spherical harmonic $Y_{m,n+m}$.

long-wave variability in the Northern Hemisphere during January 1979. [See also Daley and Williamson (1985) and Straus et al. (1987), who both emphasize that it is only in the Northern Hemisphere that the observations resemble the theoretical mode.] Other modes that warrant being identified by their observed periods include the antisymmetric "10-day wave," {1, 2}, and the gravest symmetric wavenumber two mode, the "4-day wave" {2, 1}. Some observational studies go well beyond these more well-known modes. For example, Venne (1989) identifies the following modes by looking for the predicted westward propagating structures in the appropriate frequency bands: {1, 1}, {1, 2}, {1, 3}, {1, 4}, {2, 1}, {2, 2}, {2, 3}, {3, 1}, {3, 2}, {3, 3}, {4, 1}, and {5, 1}. Hamilton and Garcia (1986) provide observational evidence for some of the $n = 0$, mixed Rossby–gravity waves, specifically {2, 0} and {3, 0}.

The effects of zonally symmetric background winds on the structure of these modes have been considered by several authors using both barotropic and fully baroclinic models. In some cases these effects have led to a greater similarity with observed westward propagating features. The gravest, most rapidly propagating modes are naturally least affected by these winds. Dickinson and Williamson (1972), Kasahara (1980), and Salby (1981) compute the changes in the structure of mode {1, 1} caused by the climatological zonally symmetric wind field and find only small changes in the troposphere (although there are very substantial alterations in the middle atmosphere.) Daley and Williamson (1985), Kasahara (1980), Salby (1981), and Wu and Miyahara (1988) analyze mode {1, 3}. In northern winter, these studies predict that it will have larger amplitudes in the Northern than in the Southern Hemisphere, by at least a factor of 2.

In the current study we take the natural next step in the consideration of background influences on Rossby normal modes. We examine how these westward propagating modes are modified when one linearizes about a state resembling the zonally *asymmetric* climatological flow. Our motivation arises from the observational studies of Branstator (1987) and Kushnir (1987), who have isolated a distinctive westward propagating pattern in the low-frequency variability of the wintertime troposphere with a period of roughly 25 days. While it possesses a large wavenumber one component, the pattern has a strongly asymmetric variance, with maximum amplitude in the North Pacific. Because this observed structure bears some resemblance to mode {1, 3}, we are curious about their relationship. Does mode {1, 3} evolve into such a more spatially localized pattern as one introduces zonal asymmetries into the basic state? Are observational studies that attempt to isolate mode {1, 3}, by starting with a zonal wavenumber decomposition, viewing the 25-day pattern of Branstator (1987) and Kushnir (1987) from a different perspective?

Previous investigations of barotropic normal modes in the presence of asymmetric mean states have concentrated on modes that develop because the climatological wintertime upper-tropospheric flow is barotropically unstable. The longitudinal variations of the flow, particularly $\partial U/\partial x$, play a central role in the energetics of these instabilities (Simmons et al. 1983, referred to hereafter as SWB). SWB, Zhang (1988), and others have attempted to relate these instabilities to the equivalent barotropic teleconnection patterns of low-frequency variability in the troposphere, most notably the Pacific–North American pattern and the North Atlantic oscillation. Typically, the most unstable modes on those asymmetric flows that have been studied to date show little evidence of westward propagation. In section 3, however, we demonstrate that when the stability analysis is repeated for the seasonal mean circulation observed in individual winters, there are many instances when unstable modes show clear westward propagation and have structures that resemble the pattern observed by Branstator (1987) and Kushnir (1987). One particularly notable example of this is the winter of 1979/80, for which a westward propagating mode stands out clearly as the most unstable. This happens to be a year in which the amplitude of the "25-day pattern" is especially strong.

In section 4 we investigate the structure of Rossby normal modes in climatological basic states. We attempt to determine which Rossby modes should be thought of as distinct from the westward propagating unstable modes. Evidence comes from continuously changing the background state from one of rest to an observed time mean asymmetric flow and identifying those modes of the resting state that can be tracked, with modest changes in structure, to modes of the observed flow. Those modes that are insensitive to the background flow can be considered to be the Rossby normal modes that retain their identity in the presence of stationary waves. Similarly, using the flow from individual winters, like 1979/80, we ask whether the dominant unstable mode from an observed flow can be tracked back to mode {1, 3} of the resting state or perhaps to some other mode. Finally, we trace the evolution of the archetypical teleconnection mode of SWB as the basic state is gradually modified to determine whether it is related to any of the other modes we examine. In this way we attempt to unify the framework in which classical external Rossby modes, unstable external westward propagating modes, and external quasi-stationary teleconnection modes are found and to determine how these three types are interrelated.

2. The model

We use the simplest nondivergent barotropic model for our investigation. The choice of a barotropic, rather than fully baroclinic, model is based on the large number of eigenvalue calculations required for this study

TABLE 1. Period and e-folding time in days for modes of the nondivergent barotropic vorticity equation linearized about November–March mean 300-mb streamfunction for various years. Second and third columns are for fastest-growing modes. Fourth and fifth are those modes to which the most unstable mode of SWB tracks. (The asterisk denotes modes used to construct CEOF1 of Fig. 1; "same" indicates that the continuation of the most unstable SWB mode matched the most unstable mode for that winter.)

	Most unstable		Continuation of SWB1	
Year	Period	e-folding time	Period	e-folding time
1976/77	24.3	8.5*	same	same
1977/78	19.2	13.3*	40.0	15.4
1978/79	42.6	7.4*	same	same
1979/80	26.4	7.6*	same	same
1980/81	31.4	11.8*	same	same
1981/82	119.0	12.0	34.5	17.2
1982/83	∞	8.0	42.8	58.5
1983/84	∞	7.2	172.9	64.8
1984/85	30.1	6.8*	29.4	8.0
1985/86	45.5	6.0*	same	same
1986/87	30.5	7.3*	same	same
1987/88	23.2	7.8*	same	same
1988/89	∞	8.0	43.9	11.1
1989/90	336.1	11.0	same	same
1990/91	39.7	11.6*	same	same

and the extra difficulty of tracking modes, as one varies a parameter, in the presence of the plethora of baroclinic modes. The choice of a *nondivergent* barotropic model, which was made to facilitate comparisons with SWB, also requires comment, since a shallow water model with an equivalent depth of 10 km is the appropriate model for external modes on a state of rest. For a resting basic state, a nondivergent model distorts the structure of the Rossby modes somewhat and artificially increases their westward phase speed, although the divergence has a smaller effect on low-frequency modes. The quasi-geostrophic external mode dispersion relation in vertical shear (Held et al. 1985) warns us, in any case, that one cannot justify the choice of a single equivalent barotropic level independent of frequency. Therefore, for the purpose of computing the effects of mean flow on these waves, the arbitrariness in the choice of the level makes the nondivergent and shallow water models equally suspect. As explained in section 4b, we also have performed a few calculations using a quasi-geostrophic spherical model with different deformation radii as a probe of the robustness of our conclusions, but fully baroclinic calculations in some future study will be required for more definitive results.

Our model is discretized in terms of a spherical harmonic basis that is truncated triangularly at 21. A biharmonic diffusion term with coefficient 2×10^{16} $m^4 s^{-2}$ is added to control the fine scales. The eigenvectors and values for the model are calculated using standard EISPACK routines.

3. Westward propagating unstable modes

Branstator (1987) suggested that recurring westward propagating barotropic features whose zonal structure is not a simple harmonic might be modes of a linear system that is influenced by the stationary waves. Because these features are prominent in nature, one might expect them to correspond to rapidly growing modes of the system. However, past instability studies have found no such mode. While the most unstable mode analyzed by SWB for January climatological 300-mb flow was reminiscent of certain teleconnection patterns, it had no apparent westward propagation. For December–February climatological conditions, Zhang (1988) and Anderson (1991) did calculate a westward propagating unstable mode, but its period was twice that reported by Branstator (1987) and Kushnir (1987) in their observational studies. We have tried November–March climatological conditions and found a mode much like Zhang's (1988).

Simmons et al. and Anderson (1991) have reported instability calculations with the barotropic vorticity equation to be rather sensitive to reasonable changes in the basic state. For example, spectra calculated for various basic states equal to the mean states of individual winters can be qualitatively and quantitatively different. By including the effects of interannual variability in the modal calculation, we have found that unstable westward propagating modes with temporal and structural characteristics like those of the observed 25-day pattern can be produced. We have calculated the fastest growing modes for background states derived from November–March mean conditions for each of the 15 winters 1976/77 through 1990/91.[2] Based on their eigenperiods, which are listed in Table 1, these divide into two categories, those with periods longer than 100 days (and thus, essentially stationary) and those with periods less than 100 days. The average period of the ten modes in the latter category is about 29 days, which is fairly similar to the period of Branstator (1987) and Kushnir's (1987) observed pattern, especially when one considers the uncertainties in our model mentioned in section 2. Furthermore, the structures of these ten modes have a good deal in common with each other and with the observed 25-day pattern. This can be seen by using the method described in appendix A to construct synthetic data that represents an atmosphere whose evolution is completely determined by these ten modes and then performing a complex empirical orthogonal function (CEOF) analysis (Barnett 1983) of the data. Sixty percent of the variance of the synthetic

[2] All basic states used in our study are based on the 300-mb streamfunction as derived from the operational analyses of the National Meteorological Center (1976/77 through 1984/85) and the European Centre for Medium-Range Weather Forecasts (1985/86 through 1990/91).

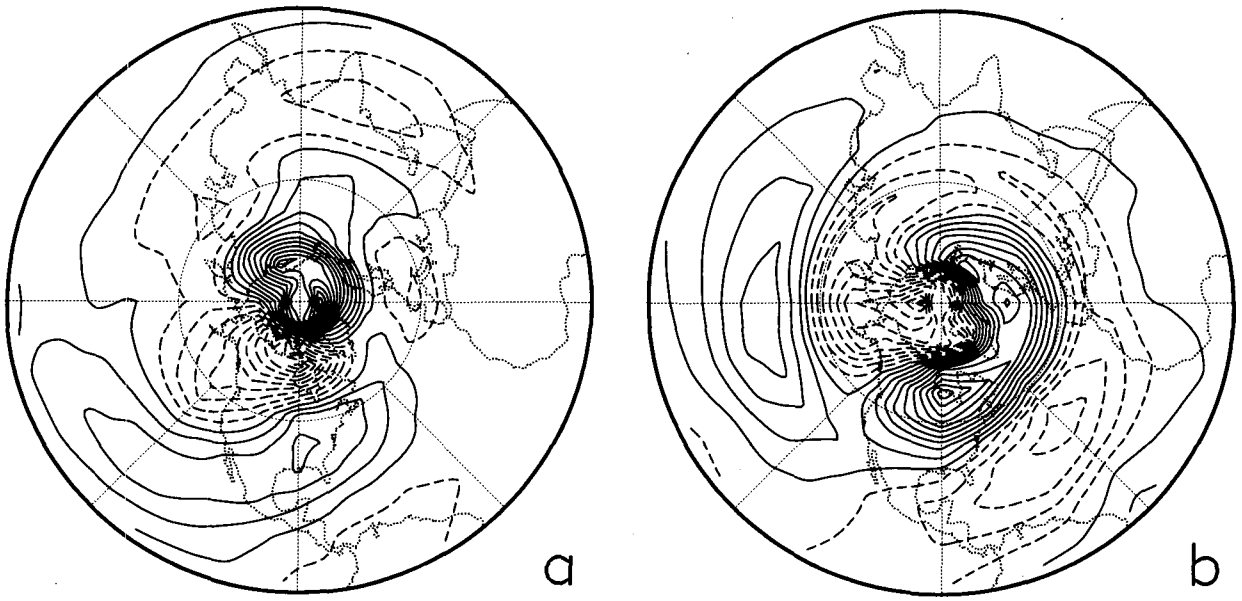

FIG. 1. Leading CEOF of data artificially generated from the ten fastest-growing modes of the nondivergent barotropic vorticity equation linearized about various November–March 300-mb streamfunction means between 1976/77 and 1990/91. Shown are two phases, separated by 90 degrees, of the CEOF. The structure in panel (a) tends to lead that in panel (b).

data can be explained by a single CEOF, which is concentrated in the Northern Hemisphere; it is shown in Fig. 1. By definition, the CEOF represents a pattern that evolves from the structure of Fig. 1a to that of Fig. 1b and then to a structure like that of Fig. 1a but of the opposite polarity, and so on. Consisting of a westward propagating disturbance whose midlatitude variance is concentrated in the Western Hemisphere, this pattern is quite similar to the observed 25-day mode. In fact, after transforming the CEOF to geopotential heights using the linear balance equation, it has a complex pattern correlation[3] of .68 with the 25-day mode that Branstator (1987) isolated from 21 winters of Northern Hemisphere analyses (his Fig. 13).

As listed in Table 1, the growth rates of the ten modes that contribute to the pattern of Fig. 1 differ by as much as a factor of two. Perhaps even more important, for certain of these winters, the growth rate of the most unstable mode is very dominant over other modes, suggesting that its role in determining the structure of that winter's long-wave variability might be more readily apparent than is typically the case. The clearest result we have obtained occurs for the winter of 1979/80. Figure 2 shows the spectrum obtained, as in SWB, by linearizing a nondivergent barotropic model about the 300-mb flow in this particular winter. A single mode stands out very clearly in the growth rate spectrum. At 7.6 days, its *e*-folding time is one-quarter that of its nearest competitor. For no other winter's basic state does the most unstable mode have such an advantage. The structure of this mode, whose variance is primarily in the Northern Hemisphere, is shown by the two streamfunction plots in Fig. 3, with (b) following (a) by one quarter period. This mode has many similarities to the CEOF of Fig. 1, which was based on ten unstable modes. It also bears a strong resemblance to a westward propagating feature that was observed during the winter of 1979/80, the winter that Branstator (1987) found to have the clearest signal of the 25-day oscillation among the many years examined. This resemblance is apparent if Fig. 3 is compared with Fig. 4, which contains the leading CEOF of twice daily 300-mb hemispheric streamfunction from this winter only. The phases, separated by one-quarter period, about 6 days, have been chosen so as to emphasize the similarity with Fig. 3. The global complex pattern correlation that measures the similarity between Figs. 3 and 4 is .61. In all three displayed renditions of this mode (Figs. 1, 3, and 4), one phase (b) resembles the PNA pattern (Wallace and Gutzler 1981), but the westward propagation in the Pacific sector is distinct from the standing structure generally associated with the PNA.

The strongly unstable, *westward propagating* modes that are captured by our barotropic model with 300-mb basic states taken from many individual winter mean flows seem to be likely counterparts to the westward propagating 25-day pattern of observations. On the other hand, in the introduction we pointed out that because of similarities in structure and timescale, the 25-

[3] The complex pattern correlation of two complex fields Φ and ψ is $[\Phi^*, \psi]/([\Phi^*, \Phi][\psi^*, \psi])^{1/2}$, where $[\cdot, \cdot]$ is the standard inner product, and the asterisk stands for complex conjugation.

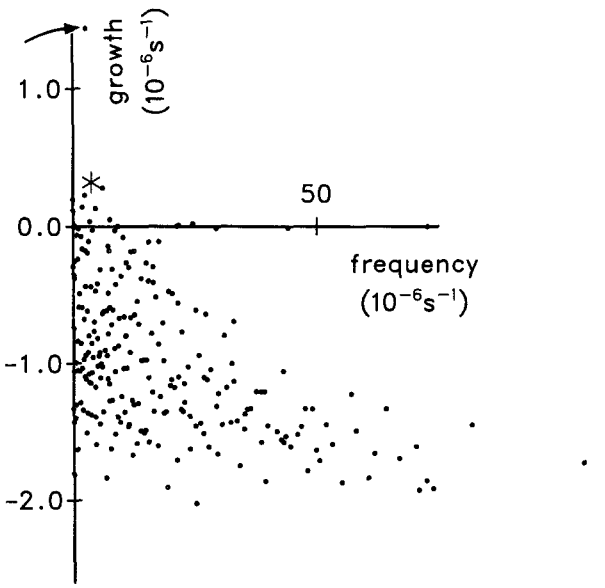

FIG. 2. Eigenspectrum of the nondivergent barotropic vorticity equation linearized about the mean Nov–Mar 1979/80 300-mb streamfunction plotted on linear scales. Real parts of eigenvalues, which represent frequency, are plotted on the abscissa, while imaginary parts, which represent growth and decay, are plotted on the ordinate. Except for pure imaginary eigenvalues, for every eigenvalue there is a corresponding one that is identical except for the sign of the real parts; these are not plotted. The asterisk indicates the eigenvalue of the mode that {1, 3} is connected to when tracked from Z to the mean of Nov–Mar 1979/80. The arrow points to the eigenvalue of the most unstable mode. One high frequency, strongly damped eigenvalue is off-scale, and not plotted.

day pattern might be related to Rossby mode {1, 3}. These two notions are not necessarily contradictory, for it may be that under the influence of the stationary waves, mode {1, 3} may become an unstable mode. In the next section we address this issue by considering how a Rossby mode changes as the basic state of the linear model is modified.

4. Mode tracking

a. Method

To determine the influence of nonresting basic states on the structure and frequency of Rossby modes, we have used a method that we refer to as mode tracking, a technique sometimes used in fluid mechanics and other fields to determine how a mode's structure is modified as one changes a system parameter. [For example, Salwen et al. (1980) employed it to find how the leading modes in Poiseuille pipe flow are affected by the Reynolds number.] One calculates the modes of a system for a series of configurations, each of which is only slightly different from its neighbors and "tracks" how the modes of interest gradually change as the system configuration is changed. In our application, we gradually change the basic state of our linear model. For example, we start with the modes of the model when it is linearized about rest and determine how they change as the basic state is gradually modified until it consists of a climatological flow. The mathematical foundation for this technique, as well as many of the difficulties that can arise, are discussed in appendix B.

To understand the workings of the procedure, consider two basic states A and B and the corresponding operators obtained by linearizing the barotropic vorticity equation about these states, L_A and L_B. One can try to identify an eigenmode of L_A with an eigenmode of L_B by computing the spectrum of $L_\epsilon = \epsilon L_A + (1 - \epsilon)L_B$ [or equivalently L_{S_ϵ} for $S_\epsilon = \epsilon A + (1 - \epsilon)B$] for values of ϵ between 0 and 1. Starting with L_A and focusing on a particular eigenvalue, one chooses a small ϵ and searches for that eigenvalue of L_ϵ closest to the eigenvalue in question. One then uses this eigenvalue as the point of comparison for the next increment in ϵ and proceeds in this way toward L_B. Increments in ϵ are chosen to be small enough that there is no danger of accidently jumping to the track of a neighboring eigenvalue. (In our case we insist that the closest eigenvalue be at least five times closer than the second closest eigenvalue at each step of the procedure. As a further guard against track jumping, we examine plots of the tracked eigenvalues and the second closest eigenvalues.) Dikiy and Katayev (1971) and Kasahara (1980) tracked several modes from a resting to a zonally symmetric state. Zhang (1988) tracked some of the most unstable modes on zonally asymmetric basic states to zonally symmetric flows.

As pointed out in the discussion in appendix B, the modes for operators L_A and L_B that mode tracking relates to each other can be path-dependent. That is, if one tracks a mode for L_A to some operator, L_C, and then continues to track that mode to L_B, there is no guarantee that the final mode in the track will be the same if one had instead tracked it from L_A to $L_{C'}$ (distinct from L_C) and on to L_B. Because of this possibility, to definitively pair eigenmodes using this procedure would require that all possible paths through basic-state phase space be considered. Not only is this impossible, but since most paths are of no physical relevance, such an all-encompassing approach would not be desirable for our purposes. For example, we consider paths through states with wind speeds orders of magnitude larger than those observed in nature to have no bearing on the issues we are interested in. Instead, as described below, whenever we wish to relate the modes for two operators, we consider several paths through phase space that we think are physically interesting. These will be paths consisting of states that are physically realizable (like observed time means), or that earlier modal studies found to be relevant to observed perturbations (like resting and zonal mean observed flows) or that are linear combinations of these two types. For some modes our results are insensitive to the paths employed. Be-

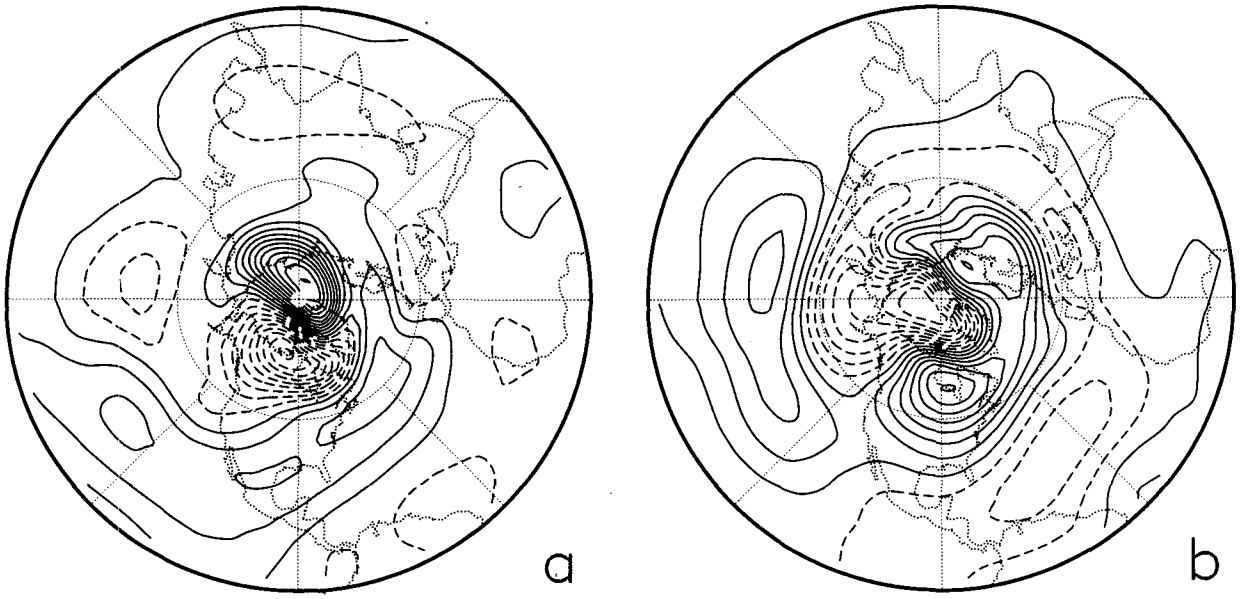

FIG. 3. Two phases of the fastest-growing eigenmode for the Nov–Mar 1979/80 300-mb basic state. The structure of (a) leads that of (b) by one-quarter period.

cause we have not tried all physically relevant paths, we cannot be certain that our results would not change if some other path were used; but since we have tried many paths, we think it is valid to consider the modes connected by these paths as being related. For other modes we find path sensitivity of varying degrees. Even in these cases we think that it is meaningful to consider two modes to be related to each other in the sense of tracking, provided one recognizes that this relationship is only valid in certain regions of phase space. The more paths that can be shown to connect two modes, the more relevant it is to consider them to be related. So, for those Rossby modes whose tracks turn out to be highly path-dependent when they are tracked from

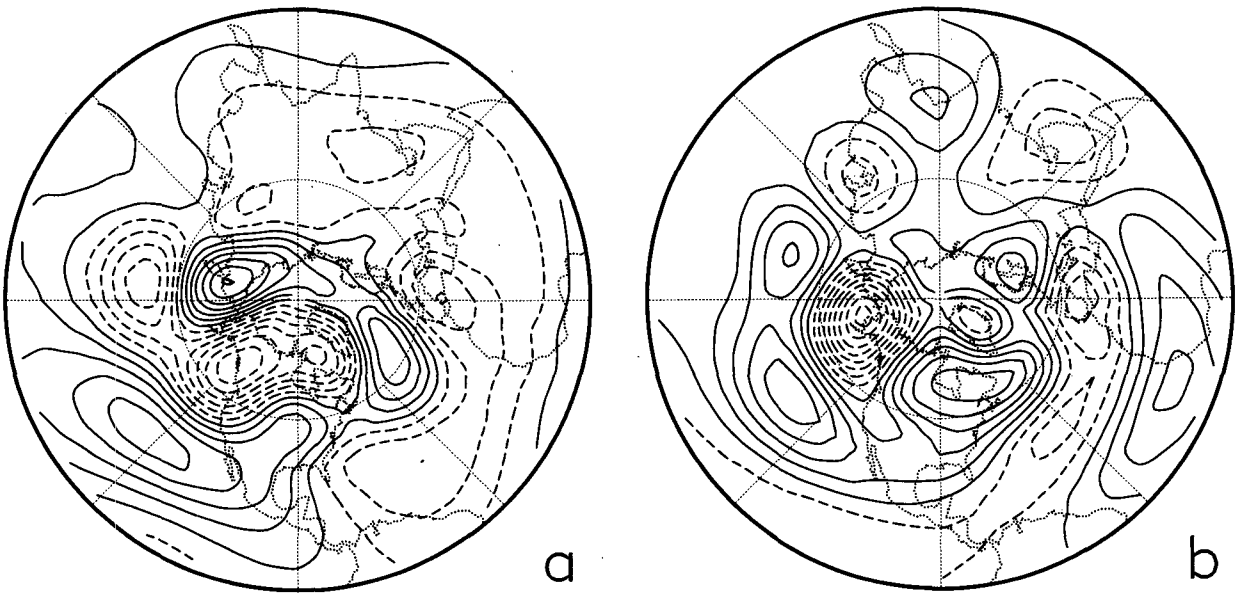

FIG. 4. Two phases, separated by 90 degrees, of the leading complex empirical orthogonal function of daily 300-mb streamfunction during Nov–Mar 1979/80. The structure in panel (a) tends to lead that in panel (b).

rest to a climatological state, the concept of Rossby normal modes in the presence of climatological waves is not very useful. For Rossby modes that are not sensitive to the path taken, it is meaningful to speak of Rossby modes in the presence of observed background waves, though their structure and frequency have been modified. In some cases the concept of a contorted mode may only make sense for sectors of phase space.

b. *Rossby mode tracks*

Figure 5a shows the eigenspectrum of the nondivergent barotropic vorticity equation linearized about a state of rest (state Z). The imaginary part of the eigenvalues, which represents growth or decay and is plotted on the ordinate, is due to the presence of diffusion, which separates modes with different values of n. The wavenumber-one 5-, 10-, and 16-day modes—{1, 1}, {1, 2}, and {1, 3}—are marked by asterisks. Figure 5b is an analogous plot when the basic state is the climatological 300-mb streamfunction averaged over the months November–March (state W). Note the very different character of this spectrum from that for the resting state: modes with substantial growth rates appear and strongly damped high-frequency modes are present. Using the procedure outlined above, we have tracked modes {1, 1}, {1, 2}, and {1, 3} of Fig. 5a to the modes marked on Fig. 5b.

Tracks of these three eigenvalues as the basic state is continuously deformed from Z to W are shown in Fig. 6. We first introduce the zonal mean flow, without any zonal asymmetries; this produces a shift in frequencies of the modes, but no growth or decay. Introducing the zonal asymmetries, mode {1, 1} becomes very weakly unstable, while mode {1, 2} becomes weakly damped. Mode {1, 3} is weakly unstable for low amplitude asymmetries but becomes weakly stable by the time W is reached. The growth or decay is too weak to have any physical significance in any of these cases.

The structure of mode {1, 1} is only slightly affected by the mean flow. The complex correlation between its structure in states Z and W is $C = .99$. Mode {1, 2} is more significantly modified, with $C = .72$, but its unperturbed structure, zonal wavenumber one with symmetric streamfunction about the equator and one node in each hemisphere, is still evident as shown in Fig. 7.

Mode {1, 3} is more dramatically altered. Its two phases on state W are shown in Figs. 8c,d. To help appreciate how this structure emerges, we also show, in Figs. 8a,b, the corresponding plot for a basic state with the same zonal mean flow as W, but with the eddy amplitudes at 70% of their W values. The correlation

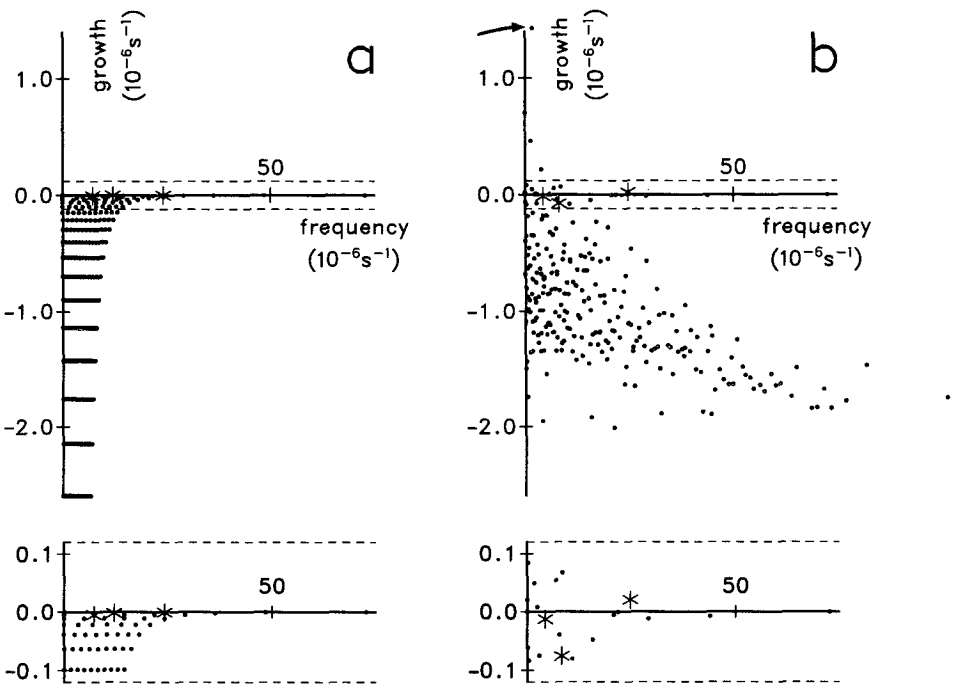

FIG. 5. Eigenspectra of the nondivergent barotropic vorticity equation linearized about (a) rest and (b) climatological Nov–Mar 300-mb streamfunction. Each is plotted on a linear scale. Asterisks indicate eigenvalues of the eigenmodes that tracking connects to modes {1, 1}, {1, 2}, and {1, 3}. Of these three, the {1, 1} mode has the highest frequency on each panel, and the {1, 3} mode has the lowest. The arrow points to the fastest-growing mode for the climatological basic state. At the bottom of each panel, the region bounded by dashed lines is reproduced with a stretched ordinate.

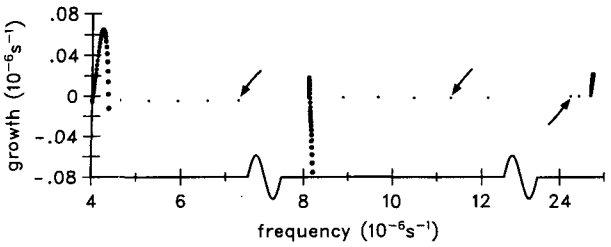

FIG. 6. Eigenvalue tracks, plotted with dots of increasing size, starting from rest (arrow), and ending at the climatological Nov–Mar 300-mb basic state for (right) the {1, 1} mode, (center) the {1, 2} mode, and (left) the {1, 3} mode. Dot spacing in these figures does not reflect the increments actually employed in the mode-tracking algorithm.

with the mode on a state of rest drops from .72 when the eddy amplitudes are at the 70% level to .61 for the full amplitudes.

Tracking all modes in this way, we find that the modes listed in Table 2 can be tracked to the climatological mean wintertime 300-mb flow, with $C > .6$. These are the Rossby modes that are distorted weakly enough that they retain their identity in the presence of climatological conditions. If, rather than tracking each of the modes in Table 2 from rest to W, we had calculated which of the W eigenvectors were strongly correlated with the 13 Z modes of Table 2, we would have matched the same pairs of modes. Thus, in spite of potential tracking difficulties like those discussed in appendix B, in these cases mode tracking has produced reasonable results. As summarized in Table 3, the effect of the nonresting basic state on the periods of these

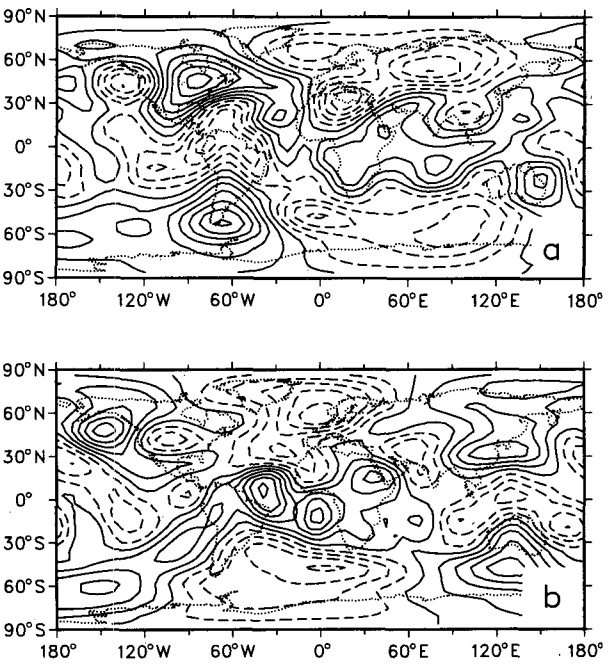

FIG. 7. Eigenmode for the climatological Nov–Mar 300-mb basic state (W) to which the mode {1, 2} tracks. Two phases of the mode, separated by 90 degrees, are shown.

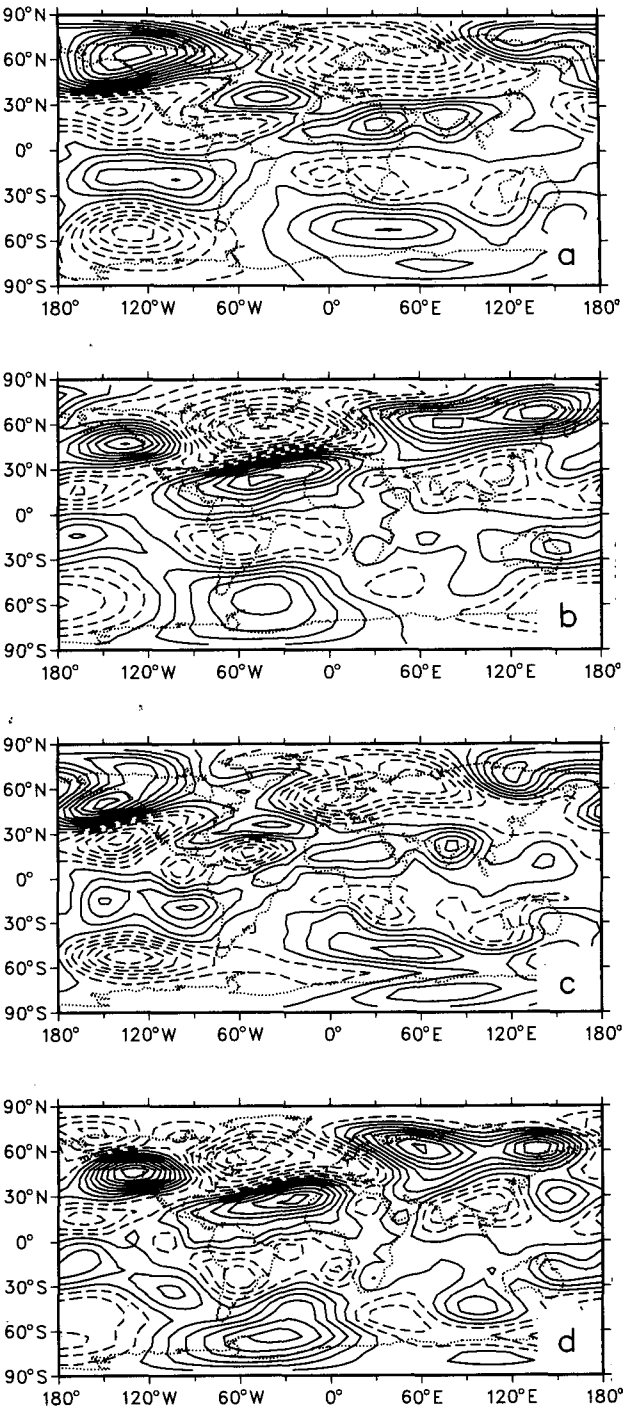

FIG. 8. Two eigenmodes in the track of the mode {1, 3} from rest to the climatological Nov–Mar 300-mb basic state (W). (a,b) Two phases of the mode when the basic-state waves have 70% of their full value. (c,d) Two phases of the mode when the basic-state waves have 100% of their full value.

modes is appreciable, especially for the lower frequency modes. The zonal mean component of W is primarily responsible for frequency shifts, just as we saw in the tracks of Fig. 6.

[As recorded in Table 2, we find that the gravest antisymmetric mode ($n = 0$) is not significantly distorted for all $m < 5$. These waves have largest amplitude in the Tropics, especially for the larger values of m. In the presence of divergence, these antisymmetric modes are mixed-Rossby gravity waves, and the nondivergent model distorts them appreciably. We do not discuss them further here.]

Most of the Rossby modes that do not meet the .6 criterion of Table 2 are related to continuum modes, a class of modes discussed in appendix B. These modes lose their identity even without the influence of basic-state asymmetries. By comparing the phase speeds of normal modes to the range of basic-state wind velocities (as in Kasahara 1980), we have found that for the zonally symmetric W background state, all but 38 of the modes are continuum modes. (This number of "discrete" modes is likely to be sensitive to resolution.) Thus, most of the eigenvalues in Fig. 2 are related to approximations to these continuum modes, which have no physical significance when considered individually. Such modes have singular structure and thus would not have structures similar to Rossby modes and, hence, do not appear in Table 2. Consequently, the basic-state asymmetries in W are at most responsible for reducing the number of modes retaining their identity from 38 to 13, the number of entries in Table 2.

TABLE 2. Information about modes of the barotropic vorticity equation that are connected by mode tracking to Rossby modes with indices m, n. "Correlation" is the complex correlation between the structure of the Rossby mode and the mode it tracks to in W. Only cases for which this correlation is greater than 0.6 are listed. "Average correlation" is the average of complex correlations between a Rossby mode and the modes it tracks to in each of 15 states based on individual winter means. Only those winters where the track continued to W end at the same mode at which a track directly from Z to W ends are included in the average. "Number of winters" is the number of winters with tracks that, when continued to W, end at the same mode as a Z to W track.

m	n	Correlation	Average correlation	Number of winters
1	0	1.00	1.00	15
1	1	.99	.99	15
1	2	.72	.63	8
1	3	.61	.41	7
2	0	1.00	1.00	15
2	1	.95	.87	13
2	2	.83	.68	11
2	3	.61	.37	5
3	0	.99	.99	15
3	1	.90	.85	7
4	0	.90	.37	13
4	1	.85	.71	10
5	0	.75	.84	12

TABLE 3. Column Z contains the periods in days of Rossby modes with indices m, n. Column [W] contains the periods of these modes when they are tracked to a basic state equal to zonal mean W. Column W contains the periods of these modes when tracked to W.

m	n	Z	[W]	W
1	0	1.0	1.0	1.0
1	1	3.0	2.9	2.9
1	2	6.0	9.0	8.9
1	3	10.0	18.2	16.6
2	0	1.5	1.7	1.7
2	1	3.0	3.3	3.3
2	2	5.0	8.7	8.4
2	3	7.5	20.2	18.7
3	0	2.0	2.5	2.5
3	1	3.3	4.6	4.6
4	0	2.4	3.5	3.5
4	1	3.8	6.8	6.8
5	0	3.0	4.5	4.2

In section 3 we noted that year to year variability in the mean circulation can appreciably affect the barotropic normal modes. As a test of the robustness of our results with the W basic state and to check for path-dependence, we have tracked each of the modes listed in Table 2 from rest to each of the mean flows from the winters of 1976/77 through 1990/91 and then on to W. The paths through phase space for these tracks consist of straight line segments from Z to the zonal mean winter mean, from there to the complete winter mean, and then to W. Entries in Table 2 report the number of such tracks that end at the same W mode at which the tracks directly from Z to W end. The larger this number, the larger the region of phase space for which the notion of that mode existing is valid. Some modes, like mode $\{1, 1\}$,[4] are completely path-independent. Others, like mode $\{1, 3\}$, are well defined less than half the time. (The winter of 1979/80 is one of the states for which mode $\{1, 3\}$ is not well defined by our criterion.) As an indication of the robustness of the structure of a mode, Table 2 lists the average complex correlation between the structure of each resting mode and the structures it tracks to in the individual winters for which the mode can be defined. Generally speaking, those modes that are found not to be definable in many winters are also strongly modified in the winters when they can be defined.

From the tracks summarized in Table 2, we can determine which of the Rossby normal modes have the potential to contribute to the observed 25-day westward propagating pattern. None of these modes tracks to the fastest-growing modes presented in section 3. In fact,

[4] Where it is unambiguous, we use the term "mode $\{m, n\}$" to refer to modes that are not Rossby normal modes of a resting state, but instead are modes of a nonresting basic state that are related to resting state mode $\{m, n\}$ by tracking.

in nearly all cases, these modes track to modes that are essentially stable, either for W or for basic states taken from individual winter means. (For example, the eigenvalue that mode {1, 3} is associated with when it is tracked from Z to the 1979/80 state is marked in Fig. 2.) Thus, they do not appear to be related to the unstable modes that we found to be structurally similar to the 25-day westward propagating pattern of observational studies. However, the modes for a given basic state are not necessarily orthogonal, so this does not preclude the possibility that one of the modes of Table 2 might also have a structure similar to the observed 25-day mode. As Branstator (1987) pointed out, the observed 25-day mode has much in common with mode {1, 3}, so we have examined it carefully.

Even if we restrict our attention to those seven winters (Table 2) when the tracks of mode {1, 3} are all related to each other, there is variability in its structure in different wintertime basic states. The leading CEOF of synthetic data constructed from the modes linked to {1, 3} for these seven winters yields the pattern of Fig. 9. It explains 52% of the variance of the synthetic data. Like the mode of Branstator (1987) and Kushnir (1987), its variance is concentrated in Northern Hemisphere high latitudes and in the Western Hemisphere. When the complex correlation between linear balanced heights for this pattern and the 25-day pattern of Branstator's Fig. 13 is calculated, it turns out to be .51. Thus, it is not as similar to the observed phenomenon as the most unstable modes (whose correlation with the observed pattern was .68). Two of these seven modes are more than marginally unstable, but the growth rate for these modes is only about one-half the growth rate of other available modes.

To check the robustness of these results, we have also performed calculations with a quasigeostrophic barotropic model with finite deformation radius. For the W basic state, one can lengthen the period of the {1, 3} mode to roughly 20 days (with the rather extreme choice of a 3000-km deformation radius), and the zonally asymmetric structure of the mode is enhanced. However, with this finite deformation radius, the {1, 3} mode, which continues to be distinct from the model's most unstable mode, is no more similar to the 25-day structure documented by Branstator (1987) and Kushnir (1987) than it was for an infinite deformation radius. Furthermore, the longer period achieved with the finite deformation radius may be invalid. In multilevel model calculations like those of Daley and Williamson (1985), where a deformation radius need not be explicitly chosen, the period of mode {1, 3} is about 17 days. As documented in Table 3, our results suggest that background waves are likely to actually shorten this period. Thus, most evidence suggests that uncertainties about the appropriate specification of a deformation radius do not influence our basic result that mode {1, 3} is distinct from the unstable barotropic modes and is not as similar to the 25-day pattern as are the unstable modes.

Based on its natural period, mode {2, 3} would seem to be the only other entry in Table 2 that might be related to the observed 25-day pattern. There are only five individual winters in which mode {2, 3} exhibits path-independence, and on average during these win-

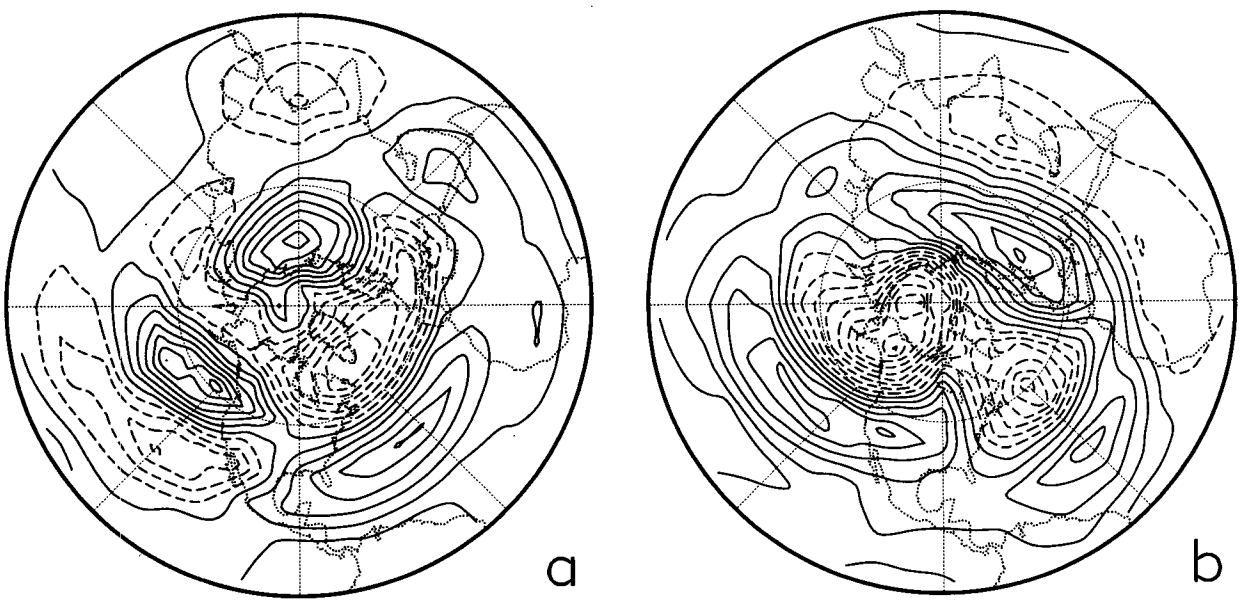

FIG. 9. Leading CEOF of data artificially generated from those seven modes to which the 16-day wave tracks for basic states representing the winters of 1980/81, 1983/84, 1985/86, 1986/87, 1987/88, 1988/89, and 1989/90.

ters, its structure is even less similar to the observations than are those modes that are related to the {1, 3} mode. For one of these five, the mode is significantly unstable and has a structure that is very similar to the 25-day mode.

c. *Unstable mode tracks*

As a final attempt to relate the 25-day pattern to Rossby normal modes, we determine whether the most unstable modes of wintertime flows that do seem to contribute to this observed pattern can be consistently tracked to any Rossby mode. When traced back to a zonally symmetric state, and then to a state of rest, these unstable modes evolve to different Rossby modes depending on which winter state is used as the initial state. Of these 16 tracks, one for each of the winters we have considered plus W, eight evolve into the continuous spectrum, three end at Rossby mode {2, 4}, two end at mode {1, 4}, two at {1, 5}, and one at {2, 3}. Though the most unstable modes on different winter mean flows track to several Rossby modes, many of them track to each other when the basic state from one winter is gradually deformed to that of another winter. Thus, links between the most unstable modes and Rossby modes are highly path dependent. The importance of the continuum also prevents us from concluding that the most unstable modes emerge from the interaction between the forced stationary waves and a small, well-defined set of Rossby–Haurwitz modes.

Although there is no single Rossby mode to which unstable modes of individual winters are always closely related, these modes *are* closely linked to a well-known eigenfunction, namely, the most unstable mode of January 300-mb climatological flow studied by SWB. As listed in Table 1, when the most unstable mode from the SWB basic state (which is based on a different dataset from that used in our winter mean states) is tracked to W and then to each of the individual winter mean states, in nine cases it ends at the most unstable mode. A cross-check of these results with the modes used to construct CEOF1 of Fig. 1 shows that 80% track to SWB's prime mode. Hence, this pattern, which we have seen may be related to the observed 25-day mode, can equally well be thought of as being the result of the most unstable modes of individual winter mean flows or as being the mode that SWB's most unstable mode evolves to under the influence of wintertime mean states.

5. Conclusions

The primary goal of our study was to determine whether the "25-day pattern" isolated by Branstator (1987) and Kushnir (1987) could be related to Rossby normal mode {1, 3}, the so-called 16-day wave, if the effects of stationary background waves on this mode were taken into account. Our results do not rule out the possibility that mode {1, 3}, as contorted by the quasi-stationary flow, may have contributed to the disturbance isolated in these studies, but they suggest that a second class of normal modes is likely to have made a contribution of at least equal importance. The westward propagating 25-day pattern is very well defined in the winter of 1979/80. A stability analysis for the 300-mb flow in 1979/80 yields a spectrum with one unstable mode distinguished clearly from all others by its large growth rate, and the structure of this mode resembles the observed 25-day pattern. For two reasons, our findings indicate this unstable mode should be considered as being distinct from mode {1, 3}. First, when the basic state is continuously modified, mode {1, 3} on a state of rest tracks to an essentially neutral mode on the 1979/80 wintertime flow. This is true for all of the paths through basic-state phase space we have tested. Second, the 1979/80 state is a flow for which mode {1, 3} is not even well defined because tracks of {1, 3} to this state are markedly path-dependent. These same facts are also basically true when 15 winter states are considered. The most rapidly growing modes for many of these states are westward propagating and have a common structure that resembles the 25-day pattern. Mode tracking provides no evidence that these unstable modes are related to the {1, 3} mode. These unstable modes then are an attractive alternative to mode {1, 3} as a theoretical counterpart to the 25-day pattern.

The evidence that unstable modes could be largely responsible for the 25-day pattern is balanced somewhat by the fact that the {1, 3} mode is near the boundary of the set of Rossby normal modes that can be tracked unambiguously to wintertime mean flows. Its structure is altered substantially, and this alteration differs from year to year. In 8 of the 15 years examined, we found evidence of path-dependence for mode {1, 3}, but for those winters when a continuation of mode {1, 3} does not seem to be path-dependent, we found its largest amplitudes were over the Western Hemisphere, just as in the 25-day pattern. Based on pattern correlations, however, it is not as similar to the 25-day pattern as are the most unstable modes, and it does not have the advantage of being strongly unstable.

In addition to structural differences, modes linked to mode {1, 3} and westward propagating unstable modes have distinct periods. For all of the winter basic states in our study, the modes that mode {1, 3} tracks to have periods between 15 and 21 days. This result is sensitive to the choice of vertical level that we have used and to the introduction of a finite-deformation radius, but based on studies with multilevel linear models, the range of periods derived in our study seems reasonable. Thus, the {1, 3} mode appears to have a characteristic timescale that is shorter than that of the observed 25-day pattern. The unstable modes on the other hand have a broad range of periods. For the 15 winter states considered, for the most part the eigenperiods were evenly distributed between 23 and 46 days. Hence, these

modes provide no explanation for the preferred 25-day timescale found by Branstator (1987) and Kushnir (1987), though Ghil and Mo's (1991) report of enhanced variance at periods of both 23 and 48 days for a similar westward propagating structure indicates that a range of periods may be consistent with observations.

Though from the standpoint of structure and instability the family of most unstable modes has some characteristics that makes it more attractive than mode {1, 3} as an explanation for the 25-day pattern of Branstator (1987) and Kushnir (1987); any observational study of large-scale westward propagating perturbations concentrated in the Western Hemisphere is likely to have contributions from both kinds of modes. If one normalizes the ten most unstable modes that contribute to the CEOF of Fig. 1 and then averages the squared spherical harmonic coefficients across those ten modes, the spatial power spectrum of Fig. 10 results. The largest value in this spectrum corresponds to the spherical harmonic that is mode {1, 3} for a resting basic state. Given this large component, as well as a near overlap in the range of periods that we found for the most unstable modes and for mode {1, 3}, most analysis techniques will not be able to separate the westward propagating modes from modes linked to mode {1, 3}. For example, Ghil and Mo (1991) found 17 and 23 days to be preferred timescales for Northern Hemisphere winter intraseasonal variability but reported the similarity in timescales hindered their efforts to separate the former signal from the data. An analysis like Madden and Speth (1989) that keys on zonal wave one might tend to emphasize mode {1, 3}, while a study like Branstator (1987) that attempts to maximize variance explained might be more influenced by the unstable modes. Indeed, such a distinction could explain the shorter timescales in the former study.

Our study finds that when linearizing about zonally asymmetric flows in a barotropic model on the sphere, there are two very distinct types of robust normal modes. As we showed in section 4, there are several modes that retain the structure and distinct westward propagation of Rossby normal modes on a resting background. The modes of this sort that we found (Table 2) are in close agreement with the Rossby and mixed Rossby–gravity modes that Venne (1989) and Hamilton and Garcia (1986) found evidence of in nature. The other type consists of the unstable modes of the kind discovered by SWB. These modes bear no simple relationship to resting state modes, at least in the sense of tracking. However, they are robust enough that they can usually be tracked from one winter's mean flow to another without exhibiting path dependence even while their phase speeds change between near stationarity and distinct westward propagation. They cannot be tracked to modes of the resting state in any simple way; indeed, they often track to the continuous spectrum if the stationary eddies are removed while retaining the zonally symmetric flow. The mode {1, 3} falls in neither of these classes. It never tracks to the most unstable mode, yet the tracking still exhibits path dependence in more than half of the cases analyzed.

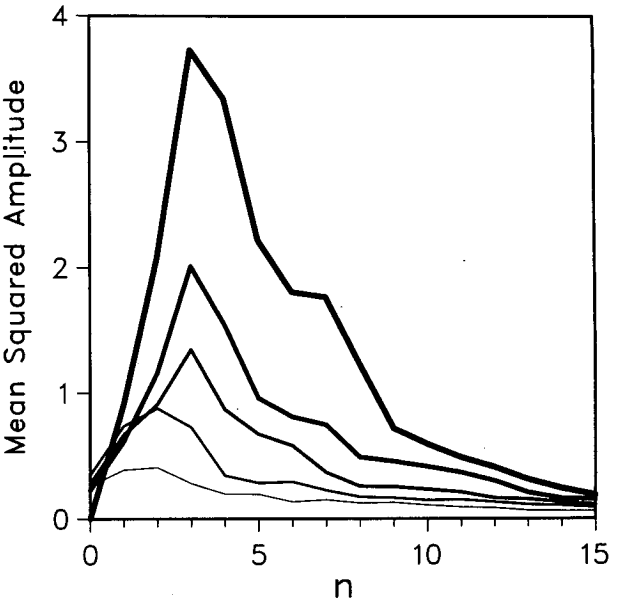

FIG. 10. Average squared amplitude as a function of Rossby mode index (n, m) (see footnote 1) for the ten fastest-growing modes used in the construction of Fig. 1. The thickest line is for $m = 1$, the second thickest line is for $m = 2$, etc.

Our results, together with those of SWB, Fredericksen (1983), and others, suggest how sensitive the structure and timescale of unstable barotropic modes can be to modifications to the background state. After all, it was because we used individual November–March means rather than climatological January means that our unstable modes tended to be westward propagating rather than quasistationary like SWB's unstable modes. Our investigation has not considered what factors determine whether the most unstable mode for a particular basic state will be westward propagating or quasi-stationary. Zhang (1988) found that quasi-stationary modes become westward propagating when he severely reduced the amplitude of basic-state waves, as expected for modes that track to the discrete rather than continuous part of the spectrum. Preliminary calculations we have performed suggest that subtler modifications to the phase and amplitude of very large scale stationary waves is enough to cause this transition. From the recent work of Nakamura (1994), we know that there does exist a strong relationship between the seasonal mean flow in a particular winter and the variance of the intraseasonal, low-frequency variability in that winter. One is tempted to try to explain this relationship by the differing barotropic instabilities of the seasonal-mean flows in different winters. We have not attempted to verify such a relationship and are wary of placing too much emphasis on the structure of the most unstable

mode in individual winters. Yet, at least in the one season for which the most unstable barotropic mode stands out most clearly from all others, namely winter 1979/80, this mode appears to leave its mark on the observed variability.

From the perspective of a modal decomposition, it is clear that there are several distinct low-frequency "modes" in the atmosphere; their structure is sensitive to the basic state, and their excitation is dependent on the details of the forcing or interaction with higher frequencies. A different perspective may result from returning to linear initial value problems with asymmetric basic states and distinguishing between those states and initial conditions that excite westward propagation versus those that excite quasi-stationary patterns. As one moves away from normal modes, however, one loses any simple capacity for explaining spectral peaks in frequency.

Acknowledgments. A. Mai made significant contributions to the project reported in this paper, including programming of the key routines, production of the figures, and insight into the behavior of the mode tracks. J. Anderson, K. Hamilton, A. Kasahara, and R. Madden carefully read and made useful comments on an earlier version of this manuscript, which was expertly prepared by L. Harper. Two anonymous reviewers have provided insight into the degree to which path dependence can affect a problem like the one we have investigated. E. Jessup pointed out to us recent developments in the application of homotopy methods to the matrix eigenvalue problem. Partial support for this research has been provided to the first author at NCAR through the National Oceanic and Atmospheric Administration under Contract NA88AANRG0140.

APPENDIX A

Synthetic Data

To make it possible to determine what structures a family of N complex eigenfunctions have in common, we construct a dataset that represents an atmosphere in which each of the family members make an equal contribution and no other patterns are present. The dataset consists of 12 000 maps. Maps $k = 1, 12\,000/N$ are equal to

$$\psi_r^{(1)} \cos \frac{\pi(k-1)}{T_1} + \psi_i^{(1)} \sin \frac{\pi(k-1)}{T_1},$$

where $\psi_r^{(1)}$ and $\psi_i^{(1)}$ are the real and imaginary parts of the first complex eigenfunction and T_1 is its natural period expressed in days. This represents the neutral evolution of the first eigenfunction. Similarly, the remaining maps are assigned values based on the neutral evolution of the rest of the N eigenfunctions. Equal contributions from the eigenvectors are assured by normalization of the eigenvectors and by letting each one contribute to the same number of maps. The number 12 000 is somewhat arbitrary but has been chosen to be large enough that each eigenvector undergoes several oscillations in the synthetic dataset. This ensures that discontinuities at the transitions points do not have a significant impact on the subsequent CEOF analysis of the synthetic data. The construction is intended to mimic a situation in which the first eigenfunction in the family dominates for a period of time and then the second eigenfunction dominates, etc. Alternatively, one can construct a dataset in which maps are calculated as the sum of the contributions from all members of the family, each mode evolving in an independent, neutral fashion. This alternative produces the same CEOFs.

APPENDIX B

Mode-Tracking Pathologies

That one is able to follow the evolution of an eigenvalue as incremental changes are made to its operator is a familiar concept in many fields and has been formalized by researchers such as Li et al. (1992), who have developed homotopy algorithms for finding the eigenvalues of real nonsymmetric matrices. Using results from algebraic function theory, for example, one can prove that if L_A and L_B are real matrices, and if one tracks an eigenvalue from L_A to L_B by considering the eigenvalues of

$$L_\epsilon = (1 - \epsilon)L_A + \epsilon L_B \qquad \text{(B1)}$$

as ϵ is varied from 0 to 1, then if the spectrum of L_A has only simple (i.e., nonrepeating) eigenvalues, the values of the eigenvalues will form piecewise smooth curves. The only places where the curve is not smooth is where that eigenvalue has multiplicity greater than 1, but this can only happen a finite number of times. Though the paths through phase space that we use in our study are, in general, functions of more than one parameter, they can all be decomposed into a few segments of the form (B1). Thus, if all eigenvalues are simple for the endpoints of these segments, then the results of Li et al. indicate that the tracks we are following are smoothly varying. Therefore, if ϵ is chosen to be small enough, we can follow the changing values of a given eigenvalue as the basic state is changed. The only exception to this will be for values of ϵ for which the track of some other eigenvalue overlaps the track we are following, but this can only happen a finite number of times. For all of the paths we consider, the eigenvalues at segment endpoints are simple (including that for a resting state because of our scale-selective diffusion), so we do not find it necessary to perturb our starting matrices, as described in Li et al., to produce well-behaved tracks.

The one difficulty that can, and does, arise in the tracking technique is that the tracks formed by different eigenvalues can coincide for a finite number of values of the parameter ϵ. This causes both practical and in-

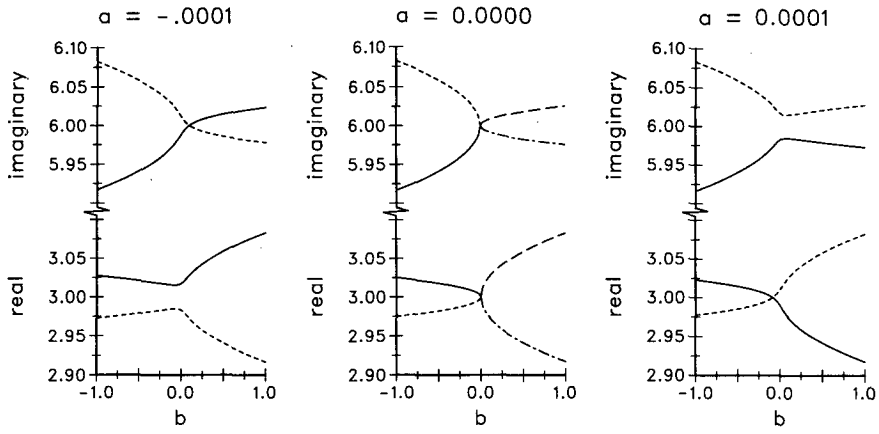

FIG. B1. Plots of the real and imaginary parts of two eigenvalues of the 4 × 4 matrix given in appendix B as a function of parameter b for three values of parameter a. Real and imaginary parts of the same eigenvalue are plotted with the same line texture (e.g., solid or dotted). In the central panel, line textures for $b > 0$ are different from those for $b < 0$ to reflect the fact that either branch is a valid continuation of the tracks through $b = 0$.

terpretive problems. Tracks are not necessarily smoothly varying at a crossing point, so following tracks in their vicinity can be hazardous. To avoid this the usual procedure is to add a small imaginary part to ϵ in the vicinity of the crossing, thus avoiding the point at which the eigenvalue has multiplicity greater than one. We rarely encounter such crossings, but when we do we simply increase ϵ slightly to pass beyond the point of crossing, make sure that no other eigenvalues are nearby, and then continue to follow both paths. (In fact, in our problems we have found crossings only when an eigenvalue coalesces with its negative conjugate pair; that is, the eigenvalue becomes pure imaginary, corresponding to formation of a stationary disturbance. Beyond the point of coalescence, the eigenvalues from the crossing tracks again split into conjugates, so it is not necessary to follow two tracks beyond the crossing since they both represent the same mode.)

Aside from track-following difficulties, the more serious problem caused by the potential for nonsimple eigenvalues is that they produce ambiguities as to which eigenvalues are related to each other in the sense of tracking. It is obvious that if one is tracking an eigenvalue and at some point the track is crossed by the track of a second eigenvalue, then beyond the crossing point a continuation down either track is equally valid. As just explained, this ambiguity in the track forces us to follow both tracks beyond a crossing point, should they not turn out to be conjugate pairs. This ambiguity is not avoided by moving into the complex plane in the vicinity of the singularity since in general tracks lead to different eigenvalues depending on which half of the complex plane the detour passes through. A more subtle and difficult problem arises because ambiguities in tracks are not just restricted to track crossings or near crossings. From perturbation operator theory (Kato 1966), it is known that if a linear operator that is a function of a complex parameter has a nonsimple eigenvalue for some value of the parameter, then if one continues an eigenvalue of that operator by changing a parameter along a path in the complex plane that encircles the point at which the eigenvalue is nonsimple, then one need not return to the same eigenvalue and mode with which one started. In general, we must pass around this point a number of times, equal to the order of the degeneracy, to return to the original mode.

Path-dependence is also seen in problems like ours where more than one real parameter is varied. (Whether one is varying one complex parameter or two or more real parameters, there are many paths that connect starting and ending values of the parameters, so in either case there is the potential for path-dependence.) A low-order example of this can be seen for the family of real matrices:

$$\begin{matrix} 6 & -5 & b & 0 \\ 5 & 6 & 10 & 0 \\ 0 & -2 & 6 & -9 \\ 0 & a & -9 & -6 \end{matrix}.$$

When a and b are both zero, this matrix has two eigenvalues equal to $3 + 6i$ and two equal to $3 - 6i$; that is, there are nonsimple eigenvalues. The center panels of Fig. B1 show the real and imaginary parts of the eigenvalues for this matrix when a is zero and b is varied between $-.01$ and $.01$. As expected from the homotopy theory, the values change smoothly as b increases from $-.01$ to near 0, so it is straightforward to track the evolution of the eigenvalues. However at 0, where the degeneracy in the eigenvalues is

present, the changes are no longer smooth, and since the real and imaginary parts of the eigenvalues coalesce simultaneously, there is no means of choosing which branch a particular path should be continued along. If a slightly different path is employed, like one for which a is held equal to $-.0001$ (left panels of Fig. B1), then unambiguous tracks can be identified. In this case, the imaginary values cross, but since the reals do not, they can be used to do the continuation. However, when a third nearby path is used, one in which a is held equal to $+.0001$ (right panels of Fig. B1), the influence of the nonsimple eigenvalue on paths with no degeneracy can be seen. In this case unambiguous paths result but the eigenvalues for $b = .01$ that are connected to the eigenvalues for $b = -.01$ are reversed from what was found for the path with a set to $-.0001$. A 4×4 matrix is the simplest that possesses such path-dependence as a function of two real parameters.

A consequence of the presence of nonsimple eigenvalues in a family of operators used in mode tracking is that if a track comes close to a point of degeneracy the structure of the associated eigenfunction can change rapidly. That this will happen can be seen from our example in Fig. B1. Once b is larger than 0, the values of the eigenvalues on the dashed line of the path with $a = +.0001$ are very similar to the values that the eigenvalues on the solid line had for the $a = -.0001$ path. Thus, their eigenfunctions also will have taken on the structure of eigenfunctions associated with the solid line of the $a = -.0001$ path. In effect, the eigenvalues and eigenfunctions will have reversed identities for b greater than 0. Craik (1985) discusses this interchange of identities that can happen if two tracks come close enough to a point of degeneracy and relates it to the coupling of modes in physical systems. Since eigenvalues can come close to each other, even if they do not coalesce, and since the consequences of jumping from one track to another are large, we have taken the precautions explained in section 4a to make sure that we do not inadvertently jump from one track to another.

One other factor that must be kept in mind while tracking is that in the presence of barotropically stable zonal shear flow for the inviscid problem, the spectrum is known to consist of neutral discrete modes, possibly infinite in number, propagating westward with respect to the mean flow at all latitudes and a continuum of singular modes with critical latitudes somewhere in the flow. For moderately viscous problems like the ones we consider, modes that are qualitatively similar to continuum modes will be present. It is possible for a discrete mode on a realistic, zonally asymmetric basic state to track to the continuum as the asymmetric part of the basic state is slowly removed. The continuum will be discretized by one's finite dimensional matrix approximation and by the introduction of dissipation, but the exact mode of the zonally symmetric state that is identified with the discrete mode of the asymmetric flow has no physical significance in this case. One can recognize this behavior by looking for singular structure in the eigenfunction or by watching for phase speeds that produce critical layers in the mean flow, as the amplitude of the stationary wave in the basic state is reduced to zero.

REFERENCES

Ahlquist, J. E., 1985: Climatology of normal mode Rossby waves. *J. Atmos. Sci.*, **42,** 2059–2068.

Anderson, J. L., 1991: The robustness of barotropic unstable modes to a zonally varying atmosphere. *J. Atmos. Sci.*, **48,** 2393–4210.

Barnett, T., 1983: Interaction of the monsoon and Pacific trade wind system at interannual timescales. Part I: The equatorial zone. *Mon. Wea. Rev.*, **111,** 756–773.

Branstator, G., 1987: A striking example of the atmosphere's leading traveling pattern. *J. Atmos. Sci.*, **44,** 2310–2323.

Craik, A. D. D., 1985: *Wave Interactions and Fluid Flows.* Cambridge University Press, 322 pp.

Daley, R., and D. Williamson, 1985: The existence of free Rossby waves during January 1979. *J. Atmos. Sci.*, **42,** 2121–2141.

Dickinson, R. E., and D. L. Williamson, 1972: Free oscillations of a discrete stratified fluid with application to numerical weather prediction. *J. Atmos. Sci.*, **29,** 623–640.

Dikiy, L. A., and V. V. Katayev, 1971: Calculation of the planetary wave spectrum by the Galerkin method. *Izv. Atmos. Oceanic Phys.*, **7,** 1031–1038.

Fredericksen, J., 1983: A unified three-dimensional instability theory of the onset of blocking and cyclogenesis. II: Teleconnection patterns. *J. Atmos. Sci.*, **40,** 2593–2609.

Ghil, M., and K. Mo, 1991: Intraseasonal oscillations in the global atmosphere. Part I: Northern Hemisphere and tropics. *J. Atmos. Sci.*, **48,** 752–779.

Hamilton, K., and R. R. Garcia, 1986: Theory and observations of the short-period normal mode oscillations of the atmosphere. *J. Geophys. Res.*, **91,** 11 867–11 875.

Held, I. M., R. L. Panetta, and R. T. Pierrehumbert, 1985: Stationary external Rossby waves in vertical shear. *J. Atmos. Sci.*, **42,** 865–883.

Kasahara, A., 1980: Effect of zonal flows on the free oscillations of a barotropic atmosphere. *J. Atmos. Sci.*, **37,** 917–929.

Kato, T., 1966: *Perturbation Theory for Linear Operators.* Springer-Verlag, 592 pp.

Kushnir, Y., 1987: Retrograding wintertime low-frequency disturbances over the North Pacific Ocean. *J. Atmos. Sci.*, **44,** 2727–2742.

Li, T. Y., Z. Zeng, and L. Cong, 1992: Solving eigenvalue problems of real nonsymmetric matrices with real homotopies. *SIAM J. Numer. Anal.*, **29,** 229–248.

Madden, R., 1979: Observations of large-scale traveling Rossby waves. *Rev. Geophys. Space Phys.*, **17,** 1935–1949.

——, and K. Labitzke, 1981: A free Rossby wave in the troposphere and stratosphere during January 1979. *J. Geophys. Res.*, **86,** 1247–1254.

——, and P. Speth, 1989: The average behavior of large-scale westward traveling disturbances evident in the Northern Hemisphere geopotential heights. *J. Atmos. Sci.*, **46,** 3225–3239.

Nakamura, H., 1994: Year-to-year and interdecadal variability in the activity of intraseasonal fluctuations in the Northern Hemisphere wintertime circulation. *J. Theor. Appl. Meteor.*, submitted.

Salby, M. L., 1981: Rossby normal modes in nonuniform background configuration. Part II: Equinox and solstice conditions. *J. Atmos. Sci.*, **38,** 1827–1840.

——, 1984: Survey of planetary-scale traveling waves: The state of theory and observations. *Rev. Geophys. Space Phys.*, **22,** 209–236.

Salwen, H., F. W. Cotton, and C. E. Grosch, 1980: Linear stability of Poiseuille flow in a circular pipe. *J. Fluid Mech.*, **98,** 273–284.

Simmons, A., J. Wallace, and G. Branstator, 1983: Barotropic wave propagation and instability, and atmospheric teleconnection patterns. *J. Atmos. Sci.*, **40,** 1363–1392.

Straus, D. M., R. S. Lindzen, and A. M. Moraes, 1987: Characteristic Rossby frequency. *J. Atmos. Sci.*, **44,** 1100–1105.

Venne, D. E., 1989: Normal-mode Rossby waves observed in the wavenumber 1–5 geopotential fields of the stratosphere and troposphere. *J. Atmos. Sci.*, **46,** 1042–1056.

Wallace, J. M., and D. S. Gutzler, 1981: Teleconnections in the geopotential height field during the Northern Hemisphere winter. *Mon. Wea. Rev.*, **109,** 785–812.

Wu, D.-H., and S. Miyahara, 1988: On the structure and behavior of transient waves during January 1979. *J. Meteor. Soc. Japan,* **66,** 247–260.

Zhang, Z., 1988: The linear study of zonally asymmetric barotropic flows. Ph.D. thesis, University of Reading, 169 pp.